INFLUENCE OF REINFORCEMENT VISCOUS PROPERTIES ON RELIABILITY OF EXISTING STRUCTURES STRENGTHENED WITH EXTERNALLY BONDED COMPOSITES

V.P. Berardi, L. Feo, G. Mancusi, M. De Piano

Department of Civil Engineering, University of Salerno, Via Giovanni Paolo II 132, 84084 Fisciano (SA), Italy, *berardi@unisa.it*, *l.feo@unisa.it*, *g.mancusi@unisa.it*, *mdepiano@unisa.it*

Keywords: *Structural strengthening, Analytical modelling, FRP, Rheological properties, Creep, Stress transfer.*

ABSTRACT

The time-depending stress transfer in existing structures strengthened with externally bonded fiber reinforced polymer (FRP) systems, due to viscous effects of reinforcement, is analysed in this paper. A new modelling strategy for assessing the long-term response of these composite beams was developed, by assembling two one-dimensional components (existing structural element and external strengthening) and accounting for thin-walled sectional geometry of FRPs. Several numerical experiments dealing with FRP laminates-reinforced concrete (RC) composite beams were performed and the corresponding results were compared with the predictions of the Effective Modulus Method (EM). A relevant stress redistribution between the components of the examined strengthened structures was observed.

1. INTRODUCTION

The strengthening of existing structures with externally epoxy-bonded fiber reinforced polymer (FRP) composites is becoming an increasingly common method of structural rehabilitation of reinforced concrete (RC), steel, masonry and timber structures.

One of the most relevant topics is represented by the reliability over time of this technique under rheological effects of FRPs, because their phases (matrix and fibres) may be highly sensitive to creep phenomena.

A similar problem occurs in the case of the steel-concrete composite structures, accounting for creep phenomena in the concrete component [1],[2].

The experimental and theoretical studies available in literature on composites rheology, performed in the industrial, aeronautic or naval field [3]-[12] and in the context of civil engineering [13]-[18], show the relevance of FRPs viscous flow. Moreover, several investigations on composites systems also highlight significant stress variations over time due to creep behavior of materials based on polymers [19]-[24].

International guidelines and technical codes introduce useful stress limitations in order to assess the safety of composite structures under viscous effects [25]-[28]. These simplified verifications may lead to an oversizing of structural reinforcement in the design process.

A similar result of FRP oversizing may be obtained via the Effective Modulus (EM) method [29], which consists of a transformation of a linear viscoelastic problem into a linear elastostatic one, under the simplified assumption of constant stress state in viscous materials during the creep flow. This hypothesis does not allow to take into account the relevant stress transfer from the FRP to the concrete core which generally reduces the viscous effects over time.

Consequently, it is interesting to study in depth the effects of these stress variations in order to get a more accurate prediction of the long-term behavior of these composite structures.

In this paper, a modelling strategy capable to evaluate the influence of rheological properties of composite materials on the mechanical behavior of strengthened existing structures is presented.
The approach is capable to evaluate the stress migration from FRP to existing structural element, also accounting for the thin-walled sectional geometry of composite. Some benchmark cases of FRP

laminates-RC composite beams are analyzed and discussed in terms of strain and stress variation over time.

The presented verification strategy offers a useful and smart tool for the reliability assessment over time of existing structures strengthened in flexure and/or in shear with composite laminates.

2. MODELLING STRATEGY

The proposed modelling strategy is based on a refinement of the mechanical model of strengthened beam proposed in [30]-[32], here extended to viscoelastic transversely isotropic materials, and is capable to account the progressive decrease of the FRP stress state over time and the thin walled sectional geometry.

2.1 KINEMATICS

Let assume a FRP laminate-reinforced concrete (RC) composite beam, as the assembly of two one-dimensional components corresponding to the concrete core ($B^{(1)}$) and to the FRP reinforcement ($B^{(2)}$)] (Figure 1).

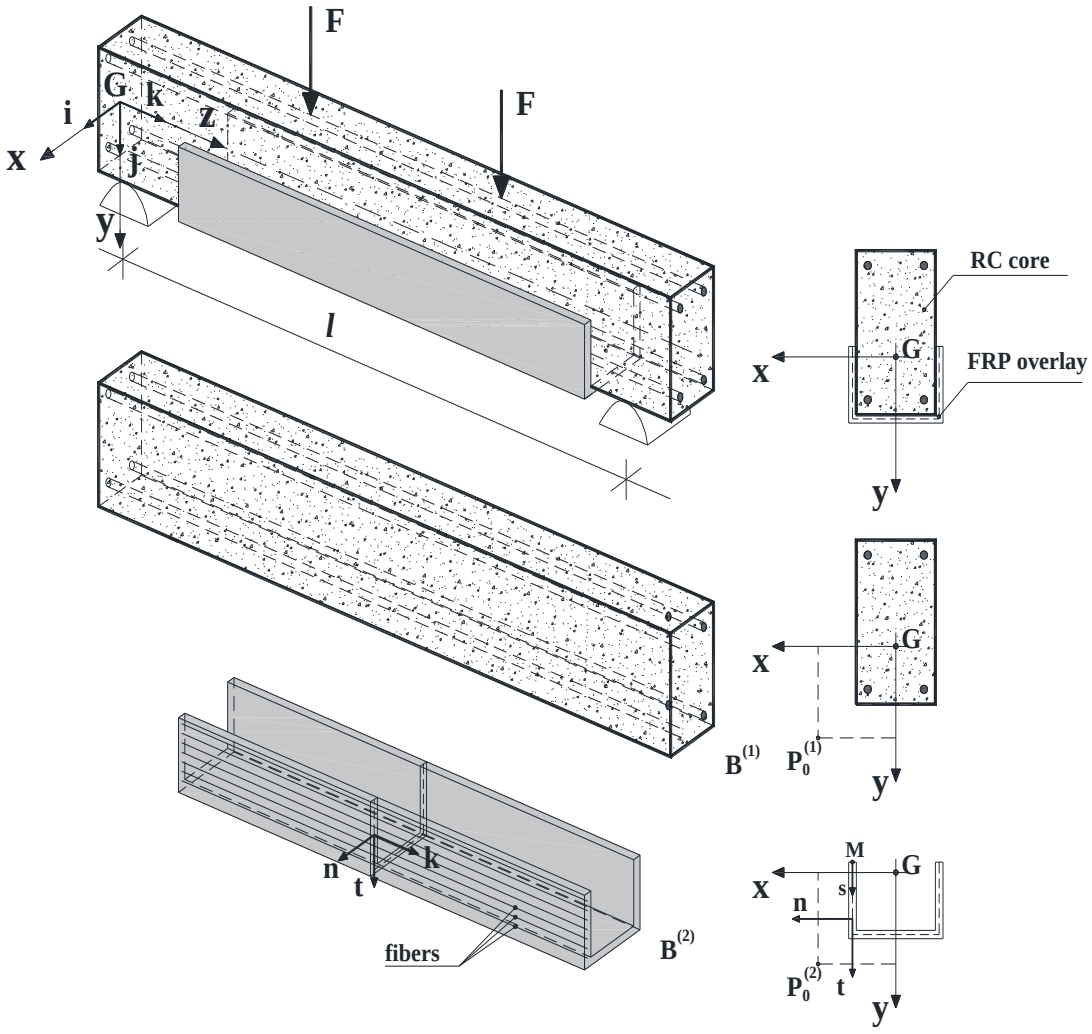

Figure 1. RC beam strengthened both in flexure ad in shear with a unidirectional FRP composite.

The concrete core behaves as a Timoshenko's beam and, then, its kinematics consists of a rigid transformation of the cross-section in its own plane and out of the same plane.

The corresponding displacement components $u^{(1)}$, $v^{(1)}$, $w^{(1)}$ of a generic point P along the coordinate *x*, *y* and *z* axes are expressed as follows:

$$u^{(1)}(y,z) = u_0^{(1)}(z) - \theta^{(1)}(z)\cdot\left(y - y_0^{(1)}\right), \tag{1a}$$

$$v^{(1)}(x,z) = v_0^{(1)}(z) + \theta^{(1)}(z)\cdot\left(x - x_0^{(1)}\right), \tag{1b}$$

$$w^{(1)}(x,y,z) = w_0^{(1)}(z) + \varphi^{(1)}(z)\cdot\left(y - y_0^{(1)}\right) - \psi^{(1)}(z)\cdot\left(x - x_0^{(1)}\right), \tag{1c}$$

being:

- $x_0^{(1)}$, $y_0^{(1)}$ the coordinates of a point $P_0^{(1)}$ of the *x*-*y* plane assumed as pole of the rigid transformation of the generic cross-section in its own plane;
- $u_0^{(1)}$, $v_0^{(1)}$, $w_0^{(1)}$ the displacement components of $P_0^{(1)}$;
- $\varphi^{(1)}$, $\psi^{(1)}$ the rigid rotations of the cross-section about *x* and *y* axes, respectively;
- $\theta^{(1)}$ the twisting rotation about the pole $P_0^{(1)}$.

The FRP overlay is modelled by means of the thin-walled beam model proposed in [31], based on a generalization of the Vlasov's theory, that consists of a rigid transformation of the cross-section in its own plane and of a warping out of the same plane.

The corresponding displacement components $u^{(2)}$, $v^{(2)}$, $w^{(2)}$ of a generic point P along the coordinate *x*, *y* and *z* axes are reported as follows:

$$u^{(2)}(s,z) = u_o^{(2)}(z) - \theta^{(2)}(z)\cdot\left(y(s) - y_o^{(2)}\right), \tag{2a}$$

$$v^{(2)}(s,z) = v_o^{(2)}(z) + \theta^{(2)}(z)\cdot\left(x(s) - x_o^{(2)}\right), \tag{2b}$$

$$w^{(2)}(s,z) = w_o^{(2)}(z) + \varphi^{(2)}(z)\cdot y(s) - \psi^{(2)}(z)\cdot x(s) + \\ -\dot{\theta}^{(2)}(z)\cdot\omega(s) + \gamma_i(z)\cdot\int_M^P f_i^*(s)\,ds, \tag{2c}$$

where:

- $x_0^{(2)}$, $y_0^{(2)}$ correspond to the coordinates of a point $P_0^{(2)}$ of the *x*-*y* plane assumed as pole of the rigid transformation of the generic cross-section in its own plane;
- $u_0^{(2)}$, $v_0^{(2)}$, $w_0^{(2)}$ are the displacement components of $P_0^{(2)}$;
- $\varphi^{(2)}$, $\psi^{(2)}$ represent the rigid rotations of the cross-section about *x* and *y* axes, respectively;
- $\theta^{(2)}$ is the twisting rotation about the pole $P_0^{(2)}$;
- $w_o^{(2)} = w_M - \varphi^{(2)}\cdot y_M + \psi^{(2)}\cdot x_M$;
- $M \equiv (x_M, y_M)$ is defined as the origin of the curvilinear coordinate *s*;
- $w_M = w^{(2)}(0,z)$
- ω is the sectorial area in the Vlasov's theory;
- $\gamma_i(z)$ $i \in \{1,2,...,N_s\}$ are the shear generalized displacement components;
- $f_i^*(s)$ are the shear shape functions given in [31].

The FRP is also considered to be bonded to the core via continuous bilateral elastic springs (penalty approach), arranged along the directions *n, t, k* of the cartesian local reference system (Figure 2). The spring reactions give an approximation of the interfacial stresses.

The springs stiffnesses (k_i in direction i = *n*, *t*, *k*) depend on the adhesive thickness, t_b, and the corresponding Young's modulus, E_b, and the shear modulus, G_b, as follows:

$$k_n = \frac{E_b}{t_b}, \quad k_t = \frac{G_b}{t_b}, \quad k_k = \frac{G_b}{t_b}. \tag{3}$$

As the stiffness of the springs increase toward $+\infty$, the model approaches the perfect adhesion condition.

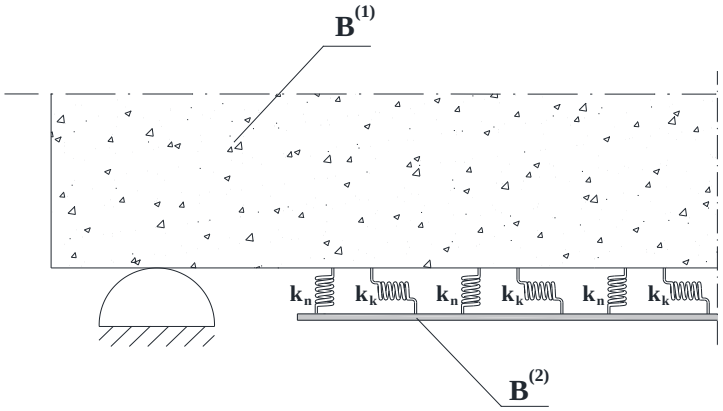

Figure 2. RC beam-FRP reinforcement interface (Section in the *yz* plane).

The hypothesis of elastic interface is justified by the international guidelines [25]-[28] that assume negligible viscous effects in the adhesive.

2.2 CONSTITUTIVE LAWS OF CONCRETE CORE MATERIALS

The concrete core is modelled by assuming a non linear constitutive law for the concrete, by considering the limited residual viscous effects in existing concretes, and a elastic-perfectly plastic constitutive law for the steel rebars

The concrete is assumed elasto-plastic in compression, according to the modified Saenz's law of Figure 3 (continuous curve), and not resistant in tension, being f_c the concrete strength in compression, ε_{c1} the concrete strain at the maximum strength point, and ε_{cu} the ultimate concrete strain.

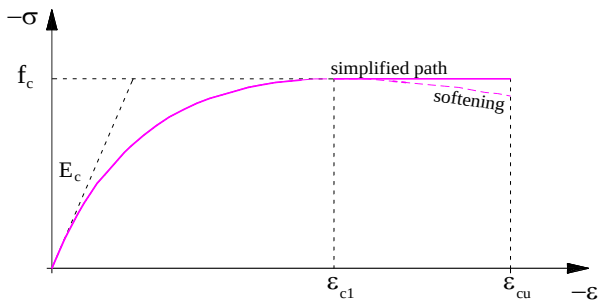

Figure 3. Modified Saenz's constitutive law.

The internal steel rebars are modelled as elastic-perfectly plastic, as illustrated in Figure 4, where f_{sy} denotes the steel yield strength, ε_{se} the strain at the yield point.

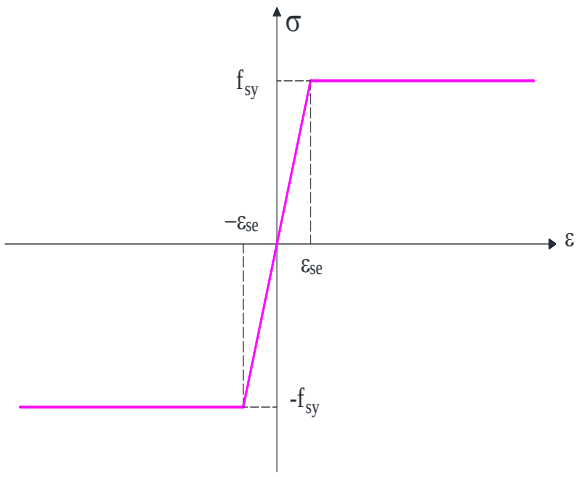

Figure 4: Elastic-perfectly plastic law for internal steel rebars.

2.3 CONSTITUTIVE LAW OF FRP REINFORCEMENT

The FRP strengthening is assumed at initial time $t = t_0$ as linear transversely isotropic and at long-term as viscoelastic transversely isotropic, by means of its instantaneous compliance matrix obtained through a finite differences approach.

At the initial time $t = t_0$ the compliance matrix $\underline{\underline{A}}$ of reinforcement does not depend on the coordinates s, n, z ($\underline{x} = (s, n, z)$):

$$\underline{\varepsilon}(\underline{x}, t_0) = \underline{\underline{A}}(\underline{x}, t_0)\underline{\sigma}(\underline{x}, t_0) = \underline{\underline{A}}\underline{\sigma}(\underline{x}, t_0), \tag{4}$$

where:

$$\underline{\varepsilon} = \begin{bmatrix} \varepsilon_1 \\ \varepsilon_2 \\ \gamma_{12} \end{bmatrix}, \quad \underline{\sigma} = \begin{bmatrix} \sigma_1 \\ \sigma_2 \\ \tau_{12} \end{bmatrix}, \quad \underline{\underline{A}} = \begin{bmatrix} \frac{1}{E_1} & -\frac{\nu_{21}}{E_2} & 0 \\ -\frac{\nu_{12}}{E_1} & \frac{1}{E_2} & 0 \\ 0 & 0 & \frac{1}{G_{12}} \end{bmatrix}. \tag{5}$$

In equation (5) the symbols "1" and "2" denote two natural axes of the material and E_i, G_{ij}, ν_{ij} are its elastic coefficients referred to the same axes.

In particular, local axis "2" is assumed aligned to global axis z (Figure 1), as frequently occurring in Civil Engineering applications.

The stress state $\underline{\sigma}(\underline{x}, t)$ in FRP, obtained by the mechanical model above presented for elastic compliance matrix, is assumed to be constant over a fixed time interval $[t_0, t_1[$ and set equal to $\underline{\sigma}(\underline{x}, t) = \underline{\sigma}(\underline{x}, t_0)$.

At the time $t = t_1$, the strain state in the overlay is updated as follows:

$$\underline{\varepsilon}(\underline{x}, t_1) = \underline{\underline{A}}^*(\underline{x}, t_1, t_0)\underline{\sigma}(\underline{x}, t_0), \tag{6}$$

where:

$$\underline{\underline{A}}^*(\underline{x}, t_1, t_0) = \begin{bmatrix} \Phi_{11}(\underline{x}, t_1, t_0) & -\Phi_{21}(\underline{x}, t_1, t_0) & 0 \\ -\Phi_{12}(\underline{x}, t_1, t_0) & \Phi_{22}(\underline{x}, t_1, t_0) & 0 \\ 0 & 0 & \Phi_{33}(\underline{x}, t_1, t_0) \end{bmatrix}, \tag{7}$$

The quantities $\Phi_{ii}(\underline{x}, t_n, t_m)$ and $\Phi_{ij}(\underline{x}, t_n, t_m)$ represent the creep compliance functions over the time interval $[t_m, t_n]$, depending on the composite viscous properties.

Within polymeric materials, these creep compliance functions are generally expressed according to either Maxwell's linear viscoelastic model or Findley's nonlinear viscoelastic model, as follows:

$$\text{Maxwell's model}\begin{cases}\Phi_{ii}(\underline{x},t_1,t_0)=\Phi_{ii}(t_1,t_0)=\left(\dfrac{1}{E_i(t_0)}+\dfrac{t_1-t_0}{\eta_{ii}}\right) & (i\ =\ 1,\ 2)\\ \Phi_{33}(\underline{x},t_1,t_0)=\Phi_{33}(t_1,t_0)=\left(\dfrac{1}{G_{12}(t_0)}+\dfrac{t_1-t_0}{\eta_{33}}\right) & \\ \Phi_{ij}(\underline{x},t_1,t_0)=\Phi_{ij}(t_1,t_0)=\left(\dfrac{\nu_{ij}}{E_i(t_0)}+\dfrac{t_1-t_0}{\eta_{ij}}\right) & (i,\ j\ =\ 1,\ 2,\ \ i\neq j)\end{cases} \tag{8}$$

$$\text{Findley's model}\begin{cases}\Phi_{ii}(\underline{x},t_1,t_0)=\left(\dfrac{\varepsilon_{0,ii}(\sigma_i\ (\underline{x},t_0))+m_{ii}(\sigma_i\ (\underline{x},t_0))(t_1-t_0)^{n,ii}}{\sigma_i\ (\underline{x},t_0)}\right) & (i\ =\ 1,\ 2)\\ \Phi_{33}(\underline{x},t_1,t_0)=\left(\dfrac{\gamma_{0,33}(\sigma_i\ (\underline{x},t_0))+m_{33}(\sigma_i\ (\underline{x},t_0))(t_1-t_0)^{n,33}}{\tau_{12}\ (\underline{x},t_0)}\right) & \\ \Phi_{ij}(\underline{x},t_1,t_0)=\left(\dfrac{\varepsilon_{0,ij}(\sigma_i\ (\underline{x},t_0))+m_{ij}(\sigma_i\ (\underline{x},t_0))(t_1-t_0)^{n,ij}}{\sigma_i\ (\underline{x},t_0)}\right) & (i,\ j\ =\ 1,\ 2,\ \ i\neq j)\end{cases} \tag{9}$$

where η_{11} and η_{22} are the viscosity in uniaxial tension creep along the 1 and 2 axes, respectively; η_{33} the viscosity in shear creep in the 1-2 plane; $\varepsilon_{0,11}$ and $\varepsilon_{0,22}$ the initial axial strains along the 1 and 2 axes, respectively; $\gamma_{0,33}$ the initial shear strains in the 1-2 plane; m_{ii} the amplitude of the transient creep strain; n,ii the time exponent, that is generally independent from the creep stress.

Many experiments have indicated that primary and secondary creep can be analysed in the field of linear viscoelasticity, as the stresses are less than forty per cent of the ultimate values of FRP.

The next step is to evaluate the stress state $\underline{\sigma}(\underline{x},t_1)$ at the time $t = t_1$, by using the updated compliance matrix $\underline{\underline{A}}(\underline{x},t_1) = \underline{\underline{A}}^*(\underline{x},t_1,t_0)$. The stress state in the FRP overlay, $\underline{\sigma}(\underline{x},t)$, is assumed to be constant in $[t_1, t_2[$: $\underline{\sigma}(\underline{x},t) = \underline{\sigma}(\underline{x},t_1)$.

At the time $t = t_2$, the total viscoelastic strains are:

$$\underline{\varepsilon}(\underline{x},t_2) = \underline{\underline{A}}^*(\underline{x},t_2,t_0)\,\underline{\sigma}(\underline{x},t_0) + \underline{\underline{A}}^*(\underline{x},t_2,t_1)\left[\underline{\sigma}(\underline{x},t_1) - \underline{\sigma}(\underline{x},t_0)\right]. \tag{10}$$

Once the total viscoelastic strains at the time $t = t_2$ are known, it is possible to update the compliance matrix $\underline{\underline{A}}(\underline{x},t_2)$ by using the following relationship:

$$\underline{\underline{A}}(\underline{x},t_2) = \underline{\underline{A}}^*(\underline{x},t_2,t_0)\ \frac{\underline{\sigma}(\underline{x},t_0)}{\underline{\sigma}(\underline{x},t_1)} + \underline{\underline{A}}^*(\underline{x},t_2,t_1)\left[1-\frac{\underline{\sigma}(\underline{x},t_0)}{\underline{\sigma}(\underline{x},t_1)}\right]. \tag{11}$$

The other steps similarly allow to update the compliance matrix in next time intervals.

The equation (11) can be generalised for the *i*-th step greater or equal to 2, as follows:

$$\underline{\underline{A}}(\underline{x},t_i) = \underline{\underline{A}}^*(\underline{x},t_i,t_0)\ \frac{\underline{\sigma}(\underline{x},t_0)}{\underline{\sigma}(\underline{x},t_{i-1})} + \sum_{k=1,i-1}\underline{\underline{A}}^*(\underline{x},t_i,t_k)\left[\frac{\underline{\sigma}(\underline{x},t_k)-\underline{\sigma}(\underline{x},t_{k-1})}{\underline{\sigma}(\underline{x},t_{i-1})}\right]. \tag{12}$$

Within the mechanical model above, the compliance matrix may be simply by considering the adopted one-dimensional FRP mechanical model, that only requires for long-term prediction the creep compliance functions Φ_{22} and Φ_{33}.

2.4 NUMERICAL FORMULATION

The mechanical model is discretized through a finite element code developed by the authors in [30] and here extended to viscous problem via a finite differences approach.

The code is based on Hermitian cubic polynomials of the kinematical unknowns, a nonlinear fiber element and the Newton-Raphson method [30].

3. ALGEBRIC APPROXIMATION OF VISCOUS PROBLEM

The general viscoelastic response $\varepsilon = \varepsilon(t)$ of a material due to an arbitrary load history $\sigma = \sigma(t)$ may be modelled by superimposing the effects produced by infinitesimal load steps $d\sigma(t)$ (Figure 5), as follows:

$$\varepsilon(t) = \sigma(t_0)\Phi(t,t_0) + \int_{t_0}^{t} \Phi(t,\tau)d\sigma(\tau)\,, \tag{13}$$

where creep function $\Phi(t, \tau)$ represents the material response at time t to a unit stress applied at time τ and held constant over the interval $[\tau, t[$.

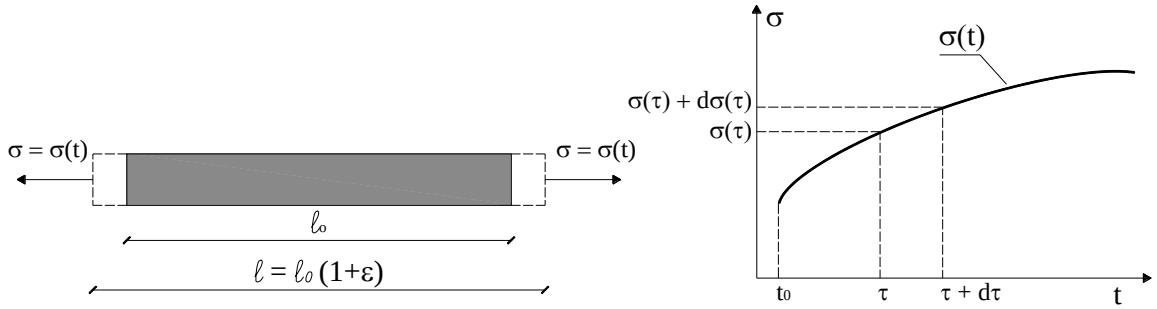

Figure 5. Sample subject to a one-dimensional load.

Usually, equation (13) is replaced by algebraic approximations, such as the well-known EM method, that is formulated as follows:

$$\begin{aligned}\varepsilon(t) &= \sigma(t_0)\Phi(t,t_0) + \int_{t_0}^{t} \Phi(t,\tau)d\sigma(\tau) = \\ &= \sigma(t_0)\Phi(t,t_0) + [\sigma(t) - \sigma(t_0)]\Phi(t,t_0) = \sigma(t)\Phi(t,t_0).\end{aligned} \tag{14}$$

The EM method transforms a linear viscoelastic problem into a linear elastostatic one, characterized by a modified Young modulus: $E(t) = 1/\Phi(t,t_0)$.

This method does not allow to evaluate the FRP stress variation and, then, may lead to an oversizing of the composite in the design process.

4. CASE STUDIES

The proposed modelling strategy was applied to RC beams strengthened in shear and/or in flexure.

The numerical simulations were referred to several RC beams, characterised by different cross-sections and span lengths, and various composite materials.

The static scheme of simply supported beam subject to two forces was considered, and the number N_s of shape functions $f_i^*(s)$ was assumed equal to 7, corresponding to a quadratic polynomial approximation of FRP shear strain [31].

The adhesive interface properties assumed in the analyses are reported in Table 1.

Table 1. Mechanical and geometrical properties of the adhesive interface.

t_b	E_b	G_b	k_n	k_t	k_k
[mm]	[N/mm^2]	[N/mm^2]	[(N/mm^3)$^{-1}$]	[(N/mm^3)$^{-1}$]	[(N/mm^3)$^{-1}$]
1.00	3600.00	1300.00	2.78E-4	7.70E-4	7.70E-4

4.1 FLEXURAL AND SHEAR STRENGTHENING

A simply supported RC beam loaded symmetrically by two forces of 10 kN and strengthened with different FRP reinforcements was analysed (Figure 6).

Different mesh sizes were considered to assess the numerical convergence of the elastic problem and the final mesh, shown in Figure 6, was used in order to ensure an optimal processing time and a good accuracy of the FEM solution. Several time increments Δt were assumed to verify the convergence of the numerical solution within the viscoelastic problem.

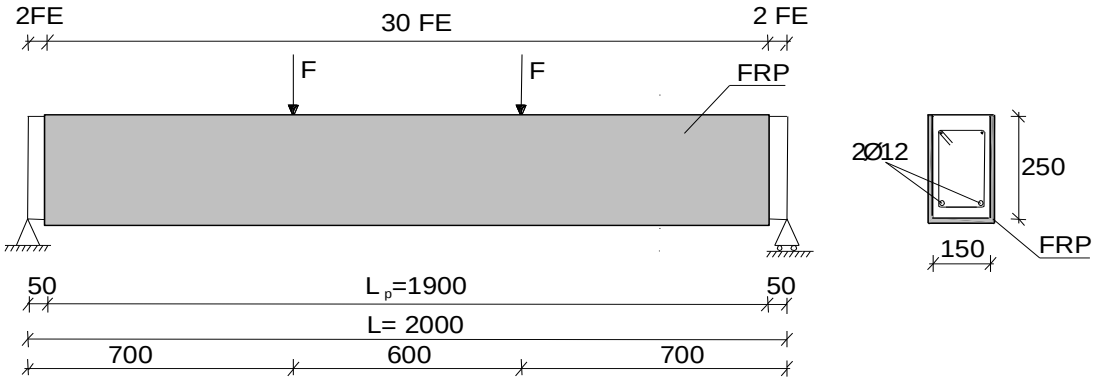

Figure 6. RC beam strengthened with FRP overlay (dimensions in mm).

Table 2 shows the mechanical properties of the concrete core constituent materials (E_c=concrete Young's modulus, E_s=steel Young's modulus of steel, ρ=steel reinforcement ratio).

Table 2. Mechanical properties of the concrete and the steel re-bars.

f_c [N/mm^2]	E_c [N/mm^2]	ε_{cu}	f_{sy} [N/mm^2]	E_s [N/mm^2]	ρ [%]
20.00	29000.00	0.0035	380.00	206000.00	1.21

The composites considered in the analysis were characterized starting from the creep tests presented in [7], [8], [9], whose corresponding fiber type, lamination and tensile strength, f_f , as well as service temperature, T, creep stress, σ_{cr}, and test time are listed in Table 3.

Table 3. Details of the specimens and the test procedure proposed in [7], [8], [9].

ID	Fibers	Lamination	f_f [MPa]	T [°C]	Test time [h]	σ_{cr} [MPa]	σ_{cr}/f_f [%]	Ref
G1	Glass	[(90/+45/-45/CM)3]s	44	21.1	25	11	25	[7]
G2	Glass	[(90/+45/-45/CM)3]s	44	65.6	25	11	25	[8]
AG	Aramid/glass	[0]	1400	20.0	50000	700	50	[8]
C1	Carbon	[(±45)2]s	168	20.0	100	70÷90	42÷54	[9]

Table 4 shows the assumed thickness, s_f, of FRPs and their viscous Maxwell's parameters obtained by the creep test data above.

Table 4. Geometric and viscous properties of the reinforcements.

ID	s_f [mm]	E_2 [N/mm^2]	G_{12} [N/mm^2]	η_{22} [N h/mm^2]	η_{33} * [N h/mm^2]	Ref
G1	6	12120	2252	5.15E+6	+∞	[7]
G2	6	10710	2252	1.18E+6	+∞	[8]
AG	1	66650	2334	2.06E+10	+∞	[8]
C1	3	20400	5200	3.00E+7	+∞	[9]

*Shear creep was considered negligible, due to lack of tests on shear creep compliance function.

A comparison between the numerical results obtained via the EM method and via the numerical procedure is presented in Table 5. The matching concerns the maximum stresses exhibited in the mid-span cross-section of the beam by the concrete, $\sigma_c(t)$, the steel, $\sigma_s(t)$, and the FRP reinforcement, $\sigma_r(t)$. The values shown refer both to the initial and to the final time t.

The relative percentage variations of stresses ($\Delta\sigma_i(t)=[\sigma_i(t)-\sigma_i(0)]/\sigma_i(0)$, $i = c, s, r$) with respect to the initial elastic solution and the percentage variations $\Delta\sigma_r(t)^{(EM)}$ between the FRP final stresses evaluated with the proposed approach and those obtained by means of the EM method, $\sigma_r(t)^{(EM)}$, are also reported in Table 5.

The results of all the samples point out relevant stress variations in the strengthened beams, which could limit the efficacy of the FRPs. In fact, the G1 specimen exhibits $\Delta\sigma_r$ = -80% for t=3000 h; the G2 specimen $\Delta\sigma_r$ = -32% for t=100 h; the AG reinforcement $\Delta\sigma_r$ = -41% after 5,7 years; and the C1 sample $\Delta\sigma_r$ = -53% for t=3000 h.

More limited variations of the stress state in the last example respect to G1 can be also observed, according to the well-known less sensitivity of carbon fibers to viscous phenomena.

Table 5. Long-term response of the strengthened RC beams.

ID	T [°C]	t [h]	Δt [h]	$\sigma_c(t)$ [N/m^2]	$\sigma_s(t)$ [N/m^2]	$\sigma_r(t)$ [N/m^2]	$\sigma_r(t)^{(EM)}$ [N/mm^2]	$\Delta\sigma_c(t)$ [%]	$\Delta\sigma_s(t)$ [%]	$\Delta\sigma_r(t)$ [%]	$\Delta\sigma_r(t)^{(EM)}$ [%]
G1	21.1	0	-	6.78	99.90	7.38	-	-	-	-	-
		3000	3000	8.15	151.50	1.40	1.40	+20	+52	-81	-
		3000	600	8.12	150.78	1.44	1.40	+20	+51	-80	2.86
		3000	300	7.72	134.46	1.46	1.40	+14	+35	-80	4.29
G2	65.5	0	-	6.92	104.60	6.81	-	-	-	-	-
		100	100	7.52	126.16	4.28	4.28	+9	+21	-37	-
		100	20	7.44	123.64	4.55	4.28	+8	+18	-33	6.31
		100	10	7.40	121.94	4.58	4.28	+7	+17	-32	7.01
AG	20.0	0	-	6.88	103.22	41.86	-	-	-	-	-
		50000	50000	7.60	129.15	23.60	23.60	+11	+25	-44	-
		50000	10000	7.57	128.05	24.24	23.60	+10	+24	-42	2.71
		50000	5000	7.56	127.82	24.28	23.60	+10	+24	-41	2.88
		50000	2500	7.56	127.80	24.29	23.60	+10	+24	-41	2.92
		50000	2000	7.56	127.80	24.30	23.60	+10	+24	-41	2.97
C1	20.0	0	-	6.97	106.41	13.19	-	-	-	-	-
		3000	3000	7.84	138.58	5.71	5.71	+12	+30	-57	-
		3000	600	7.78	136.34	6.17	5.71	+12	+28	-53	8.06
		3000	300	7.70	134.45	6.20	5.71	+10	+26	-53	8.58

4.2 FLEXURAL STRENGTHENING

Two simply supported strengthened RC beams subject to two forces of 75 kN [Figure 7] and characterized by a different cross-section and overlay [Figure 8] were analysed.

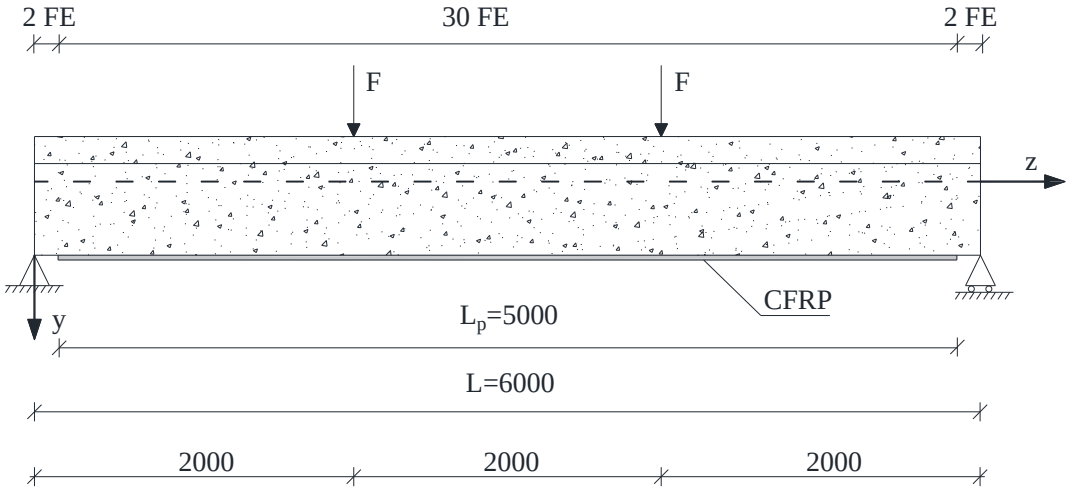

Figure 7 - RC beam strengthened with FRP overlay (dimensions in mm).

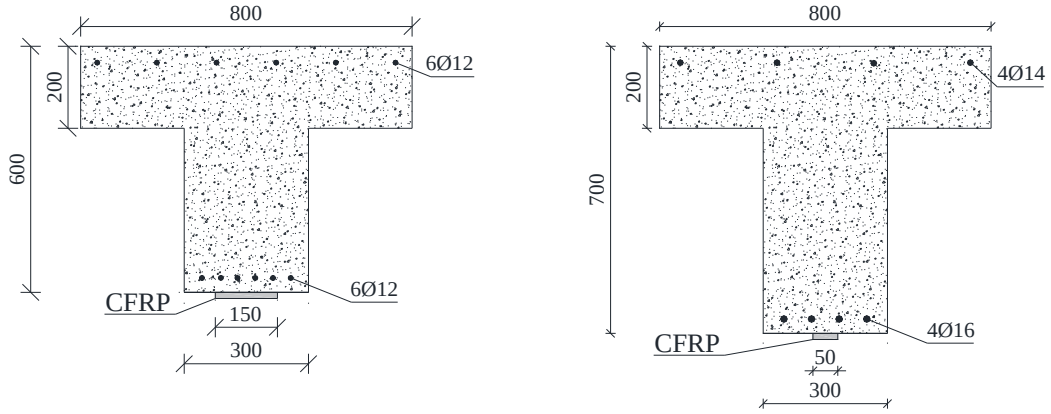

Figure 8 – Beams cross-section, C2 (left) and C3 (right) FRP configuration (dimensions in mm).

The FEM analysis was performed by considering the mesh of Figure 7, which allows an optimal processing time, as well as a good accuracy of numerical solution, as verified via the convergence test.

The corresponding mechanical properties of the concrete core constituent materials are listed in Table 6 (ρ_{c2}=steel reinforcement ratio for the C2 cross-section, ρ_{c3}=steel reinforcement ratio for the C3 cross-section).

Table 6. Mechanical properties of the concrete and the steel re-bars.

f_c [N/mm^2]	E_c [N/mm^2]	ε_{cu}	f_{sk} [N/mm^2]	E_s [N/mm^2]	ρ_{c2} [%]	ρ_{c3} [%]
17.60	27500.00	0.0035	440.00	206000.00	0.48	0.46

The thickness of the CFRP laminates was assumed equal to 1 mm and the service temperature of 25°C in both configurations.

The mechanical and Findley's rheological properties of the composite, obtained by the creep tests of [±45]4s laminated composites presented in [6], are reported in the Table 7 and refer to an expression of time in minutes.

Table 7. Viscous properties of the reinforcement.

E_2 [N/mm^2]	f_f [N/mm^2]	T [°C]	σ_{cr} [MPa]	$\varepsilon_{0,22}$	m_{22}	$n,22$
18500	315.00	25	31.46	0.0030	0.00100	0.112
			62.92	0.0096	0.006785	0.112
			94.38	0.0250	0.01250	0.112

The short and long-term shear properties of the composites were not considered, because the shear contribution of the composite is negligible, as given by the thin-walled beam model in the case of lamina.

A comparison between the numerical results obtained via the EM method and via the numerical procedure here proposed is shown in Table 8.

Table 8. Long-term response of the strengthened C2 and C3 beams.

ID	T [°C]	t [h]	Δt [h]	$\sigma_c(t)$ [N/m^2]	$\sigma_s(t)$ [N/m^2]	$\sigma_f(t)$ [N/m^2]	$\sigma_f(t)^{(EM)}$ [N/mm^2]	$\Delta\sigma_c(t)$ [%]	$\Delta\sigma_s(t)$ [%]	$\Delta\sigma_f(t)$ [%]	$\Delta\sigma_f(t)^{(EM)}$ [%]
C2	25	0	-	7.20	382.60	62.92	-	-	-	-	-
		30000	30000	10.77	382.60	29.70	29.70	+50	-	-53	-
		30000	15000	10.50	382.60	31.08	29.70	+46	-	-50	5
		30000	10000	10.48	382.60	31.85	29.70	+45	-	-49	7
C3	25	0	-	7.38	382.60	94.38	-	-	-	-	-
		30000	30000	10.80	382.60	23.00	23.00	+46	-	-76	-
		30000	15000	10.46	382.60	23.92	23.00	+41	-	-75	4.00
		30000	10000	10.37	382.60	24.86	23.00	+40	-	-74	8.08

Like the previous section, numerical simulations point out the relevant influence of the FRP rheological properties on the mechanical behavior of the plated beams.

The significant variations of the composite stress state (e.g. $\Delta\sigma_r$ =-49% for C2 and $\Delta\sigma_r$ =-74% for C3) show the inefficacy over time of the strengthening intervention.

5. CONCLUSIONS

In this paper, a modelling strategy capable to evaluate the long-term response of existing structural elements strengthened with FRP, under the rheological effects of composite, has been shown. The approach is based on a refinement of the mechanical model of strengthened beam proposed in [30]-[32] and allows to calculate the progressive variation of the stress state in overlay, taking into account the viscoelastic behavior of composite and its thin-walled sectional geometry.

Some benchmark cases of FRP laminates-RC composite beams have been developed, by considering both linear and non linear viscoelastic external reinforcements. In the first case, their viscous behavior has been modelled by means of Maxwell's law, in the second one via Findley's law.

The results obtained have shown the viscous properties of composites can relevantly influence the mechanical behavior of beams strengthened in flexure and/or in shear, according to the significant 32-76 per cent variations in the overlay stresses. The comparison between the predictions of the proposed model and those given by the EM approach have highlighted 2-9 per cent variations in the composite stresses.

The analysis has also pointed out that creep effects are very significant even if the FRP stress limitation suggested by International guidelines and technical codes, for accounting the degradation of mechanical properties of FRP-based systems due to the creep phenomena [25]-[28], are satisfied for all examined strengthened beams.

The proposed approach may represent a useful and efficient tool to predict the long-term behavior of FRP laminates-RC composite beams and needs a less computational burden than that required by either 2D or 3D FEM analysis.

Such a modelling strategy may be also easily extended to other composite systems, such as bonded joints used in new constructions made of FRP elements [33].

6. REFERENCES

[1] Price A.M., Anderson D., Composite Beams in Constructional Steel Design, Elsevier Applied Science Publishers, 4.1, 1992.

[2] Johndon R.P., Composite Structures of Steel and Concrete: Blackwell Scientific Publications, Oxford, 1994.

[3] Ferry J.D., Viscoelastic properties of polymers, J. Wiley & Sons New York, 1980.

[4] W. N. Findley, "26-year creep and recovery of poly(vinyl chloride) and polyethylene", Polym. Eng Sci., 27(8), pp. 582-585, 1987.

[5] Yen, S.-C. and Williamson, F.L., Accelerated characterization of creep response of an off-axis composite material. Compos. Sci. Technol., 38, 103-118, 1990.

[6] C.C.M. Ma, N.H. Tai, S.H. Wu, S.H. Lin, J.F. Wu, J.M. Lin, "Creep behavior of carbon-fiber-reinforced PEEK $[+/-45]_{4s}$ laminated composites", Composites: Part B, 28, 407-417, 1997.

[7] Barbero E., Harris J.S.: Prediction of creep properties from matrix creep data, Journal of Reinforced Plastics and Composites, Vol 17, No.4, 1998.

[8] Maksimov R.D., Plume E.: Long-Term creep of hybrid aramid/glass fiber-reinforced plastics, Mechanics of Composite Materials, Vol. 37, No. 4, 2001.

[9] Petermann J., Schulte K.: The effects of creep and fatigue stress ratio on the long-term behavior of angle-ply CFRP, Composite Structures, 57, pp.205-210, 2002.

[10] Rwawiire, S., Tomkova, B., Wiener, J., Militky, J., Kasedde, A., Kale, B.M., Jabbar, A. Short-term creep of barkcloth reinforced laminar epoxy composites, Composites Part B: Engineering, 103, pp. 131-138, 2016.

[11] Sá, M.F., Gomes, A.M., Correia, J.R., Silvestre, N. Flexural creep response of pultruded GFRP deck panels: Proposal for obtaining full-section viscoelastic moduli and creep coefficients, Composites Part B: Engineering, 98, pp. 213-224, 2016.

[12] Qin, Y., Fancey, K.S. Viscoelastically prestressed polymeric matrix composites – Effects of temperature on Charpy impact behaviour, Composites Part B: Engineering, 141, pp. 265-270, 2018.

[13] Ascione, F., Berardi, V.P., Feo, L., Giordano, A. An experimental study on the long-term behavior of CFRP pultruded laminates suitable to concrete structures rehabilitation, Composites Part B: Engineering 39(7-8), pp. 1147-1150, 2008.

[14] Ascione, L., Berardi, V.P., D'Aponte, A. A viscoelastic constitutive law for FRP materials, International Journal of Computational Methods in Engineering Science and Mechanics, 12 (5) 225-232, 2011.

[15] Nedjar, B. A time dependent model for unidirectional fibre-reinforced composites with viscoelastic matrices. International Journal of Solids and Structures 48(16-17), pp. 2333-2339, 2011.

[16] Ascione, L., Berardi, V.P., D'Aponte, A. Creep phenomena in FRP materials, Mechanics Research Communications, 43, pp. 15-21, 2012.

[17] Nedjar, B. Modeling long-term creep rupture by debonding in unidirectional fibre-reinforced composites. International Journal of Solids and Structures 51(10), pp. 1962-1969, 2014.

[18] Berardi, V.P., Perrella, M., Feo, L., Cricrì, G. Creep behavior of GFRP laminates and their phases: Experimental investigation and analytical modelling, Composites Part B: Engineering, 122, pp. 136-144, 2017.

[19] Triantafillou T.C., Plevris N.: Time-dependent behavior of RC members strengthened with FRP laminates, Journal of Structural. Engineering, 120(3), 1994.

[20] Ascione, L., Berardi, V.P., D'Aponte, A. Long-term behavior of PC beams externally plated with prestressed FRP systems: A mechanical model. Composites Part B: Engineering 42(5), pp. 1196-1201, 2011.

[21] Berardi, V.P., Mancusi, G. Time-dependent behavior of reinforced polymer concrete columns under eccentric axial loading. Materials 5(11), pp. 2342-235, 2012.

[22] Mancusi, G., Spadea, S., Berardi, V.P. Experimental analysis on the time-dependent bonding of FRP laminates under sustained loads. Composites Part B: Engineering, 46, pp. 116-122, 2013.

[23] Berardi, V.P., Mancusi, G. A mechanical model for predicting the long term behavior of reinforced polymer concretes. Mechanics Research Communications 50, pp. 1-7 47, 2013.

[24] Emara, M., Torres, L., Baena, M., Barris, C., Moawad, M. Effect of sustained loading and environmental conditions on the creep behavior of an epoxy adhesive for concrete structures strengthened with CFRP laminates, Composites Part B: Engineering, 129, pp. 88-96, 2017.

[25] CEB-FIP, Externally bonded FRP reinforcement for RC structures, 2001.

[26] JSCE, Recommendation for design and construction of concrete structures using continuous fiber reinforcing materials, 2007.

[27] CNR-DT 200 R1, Guide for the Design and Construction of Externally Bonded FRP System for Strengthening Existing Structures, 2013.

[28] ACI Committee 440, Guide for the design and construction of externally bonded FRP systems for strengthening concrete structures, 2017.

[29] CEB-FIP, Manual on Structural Effects of Time-Dependent Behavior of Concrete, Bullettin d'Information n. 142-142bis, 1984.

[30] Ascione, L., Berardi, V.P., Feo, L., Mancusi, G. A numerical evaluation of the interlaminar stress state in externally FRP plated RC beams. Composites Part B: Engineering 36(1), pp. 83-90, 2005.

[31] Feo, L., Mancusi, G. Modeling shear deformability of thin-walled composite beams with open cross-section, Mechanics Research Communications 37(3), pp. 320-325, 2010.

[32] Feo, L., Mancusi, G. The influence of the shear deformations on the local stress state of pultruded composite profiles. Mechanics Research Communications 47, pp. 44-49, 2013.

[33] Orefice, A., Mancusi,G., Berardi V.P., Feo L., Zuccaro G. Residual stiffness of bonded joints for fibre-reinforced polymer profiles. Composites Part B: Engineering, 144, pp.237-253, 2018.